

Electronic Supplementary Information

Imidazolium-based Ionic Polyurethanes with High Toughness, Tunable Healing Efficiency and Antibacterial Activities

Ning Duan, Zhe Sun, Yongyuan Ren, Ziyang Liu, Lili Liu, and Feng Yan*

Department of Polymer Science and Engineering, College of Chemistry, Chemical Engineering and
Materials Science, Soochow University, Suzhou, 215123, China.

E-mail: fyan@suda.edu.cn

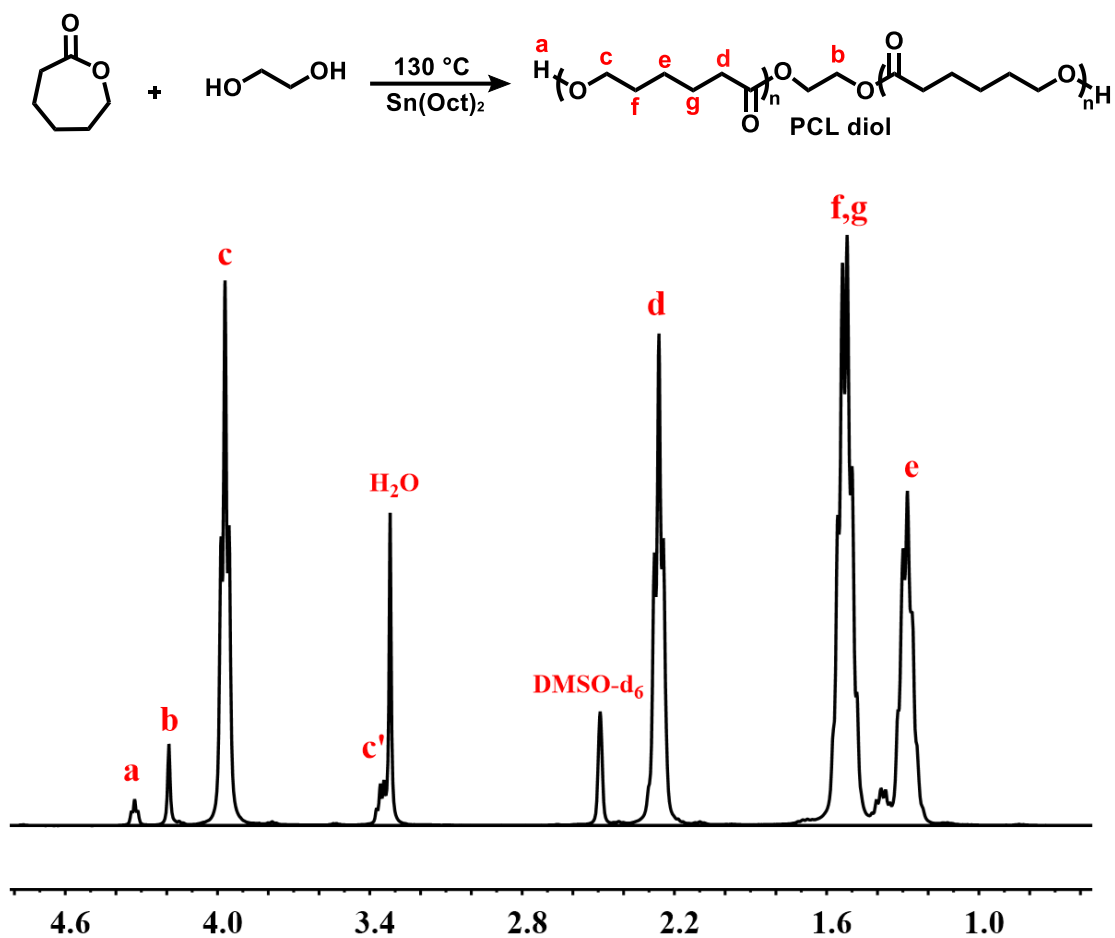
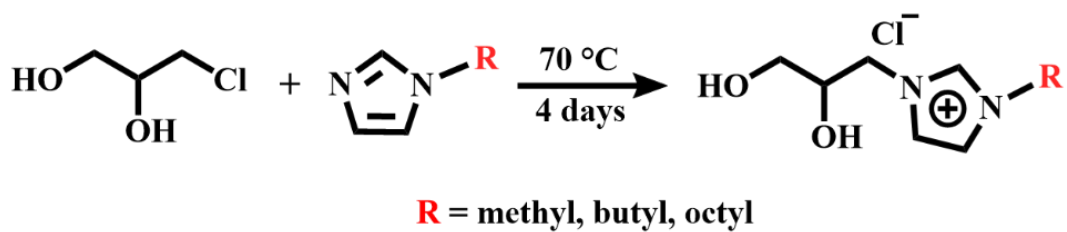


Fig. S1. ^1H NMR spectrum of PCL in DMSO-d_6 (400 MHz).



Scheme S1. Synthesis procedure for the imidazolium ionic liquid diol

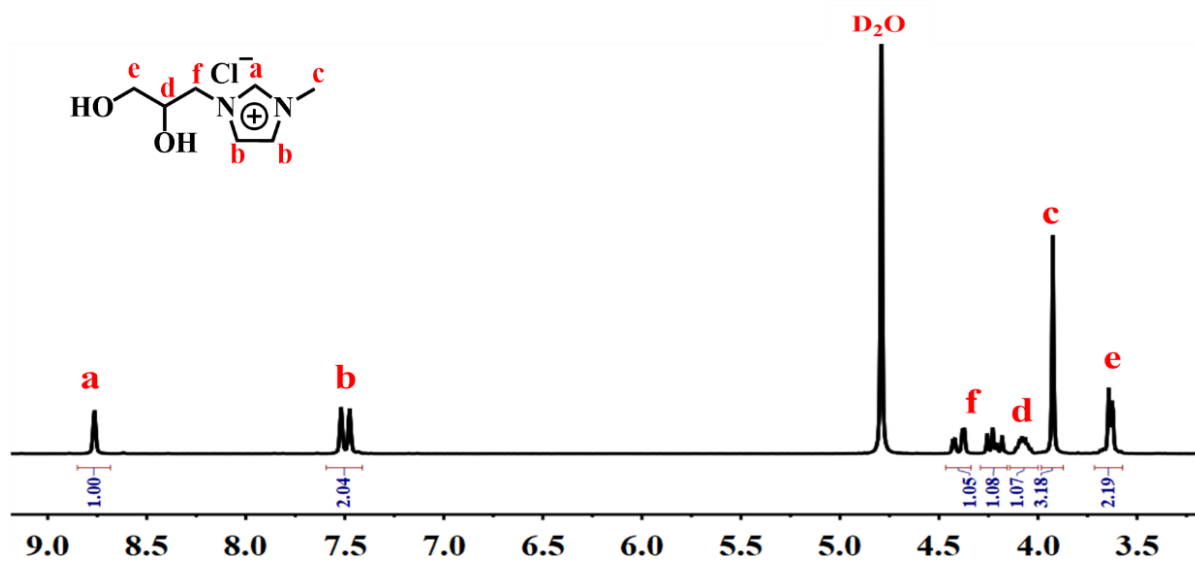


Fig. S2. ¹H NMR spectrum of [MIM_{1,g}]⁺Cl⁻ in D₂O (400 MHz).

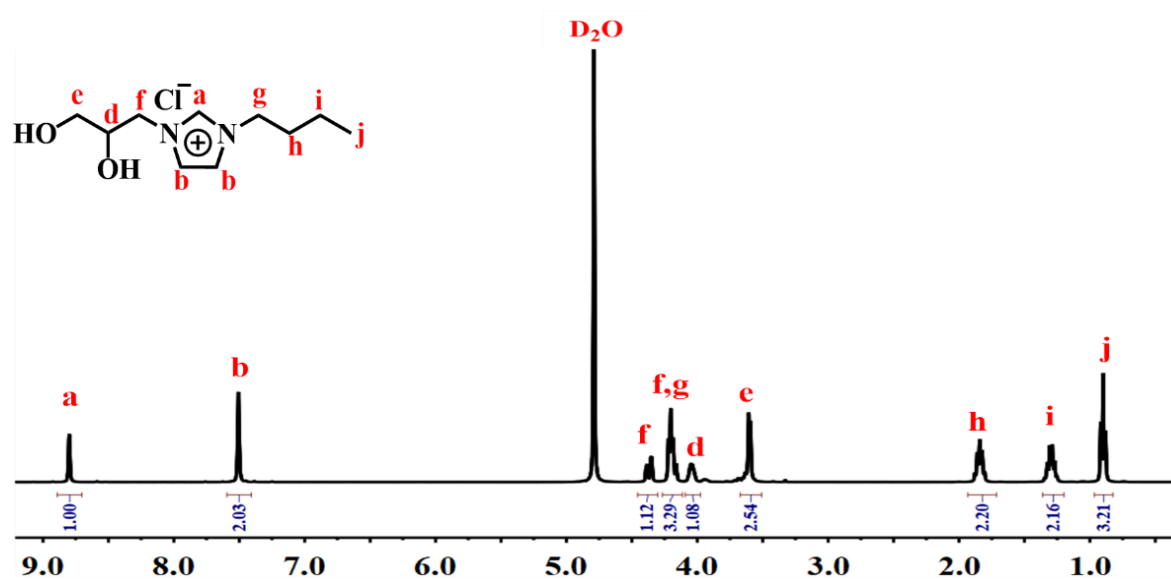


Fig. S3. ¹H NMR spectrum of [BIM_{1,g}]⁺Cl⁻ in D₂O (400 MHz).

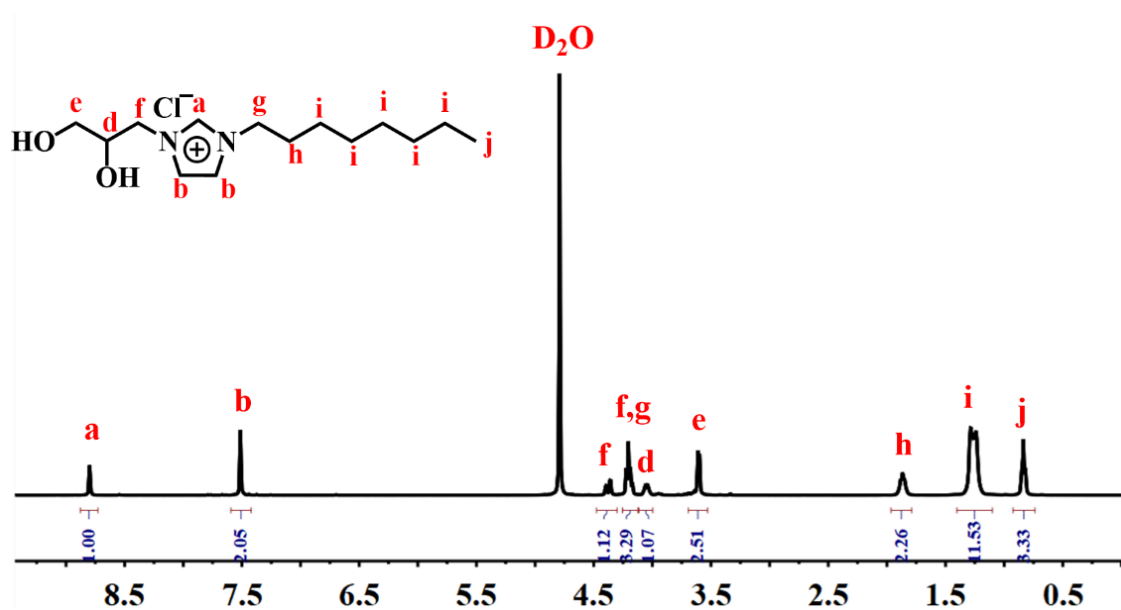


Fig. S4. ¹H NMR spectrum of [OIM_{1,g}]⁺Cl⁻ in D₂O (400 MHz).

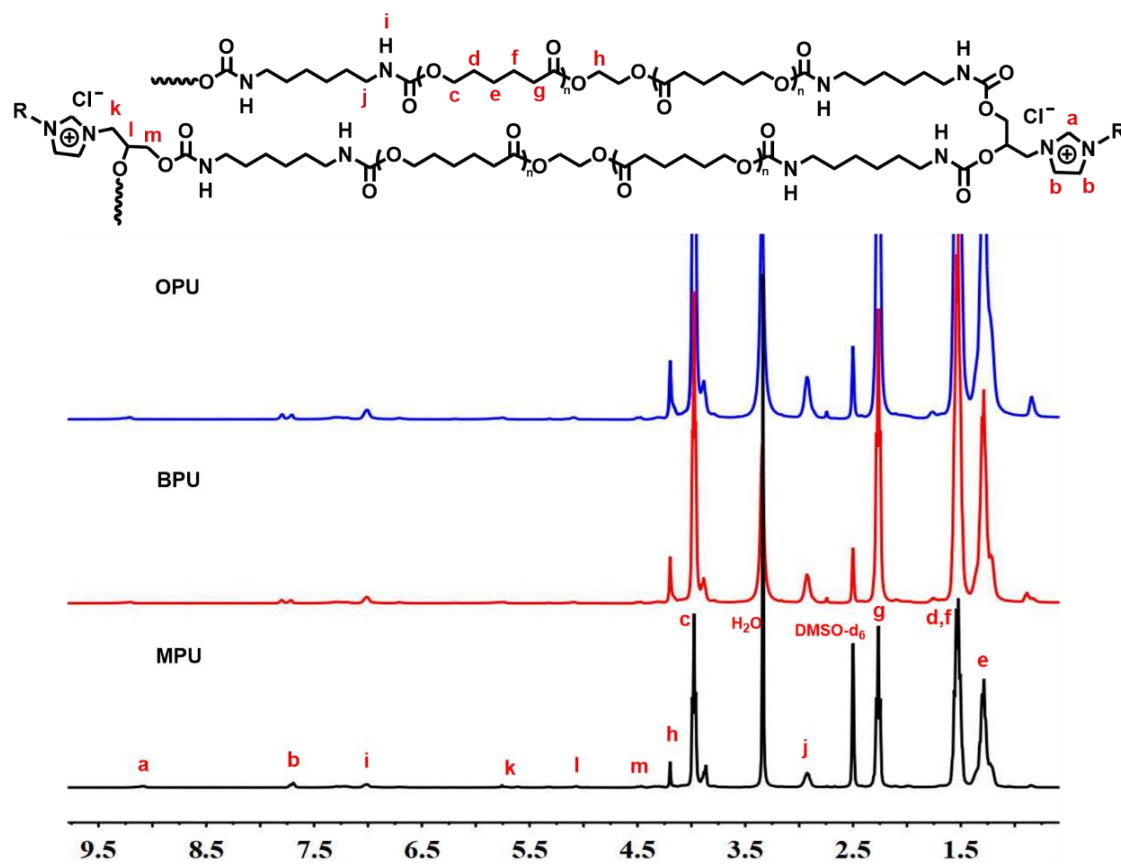


Fig. S5. ¹H NMR spectra of MPU, BPU, and OPU in DMSO-d₆ (400 MHz).

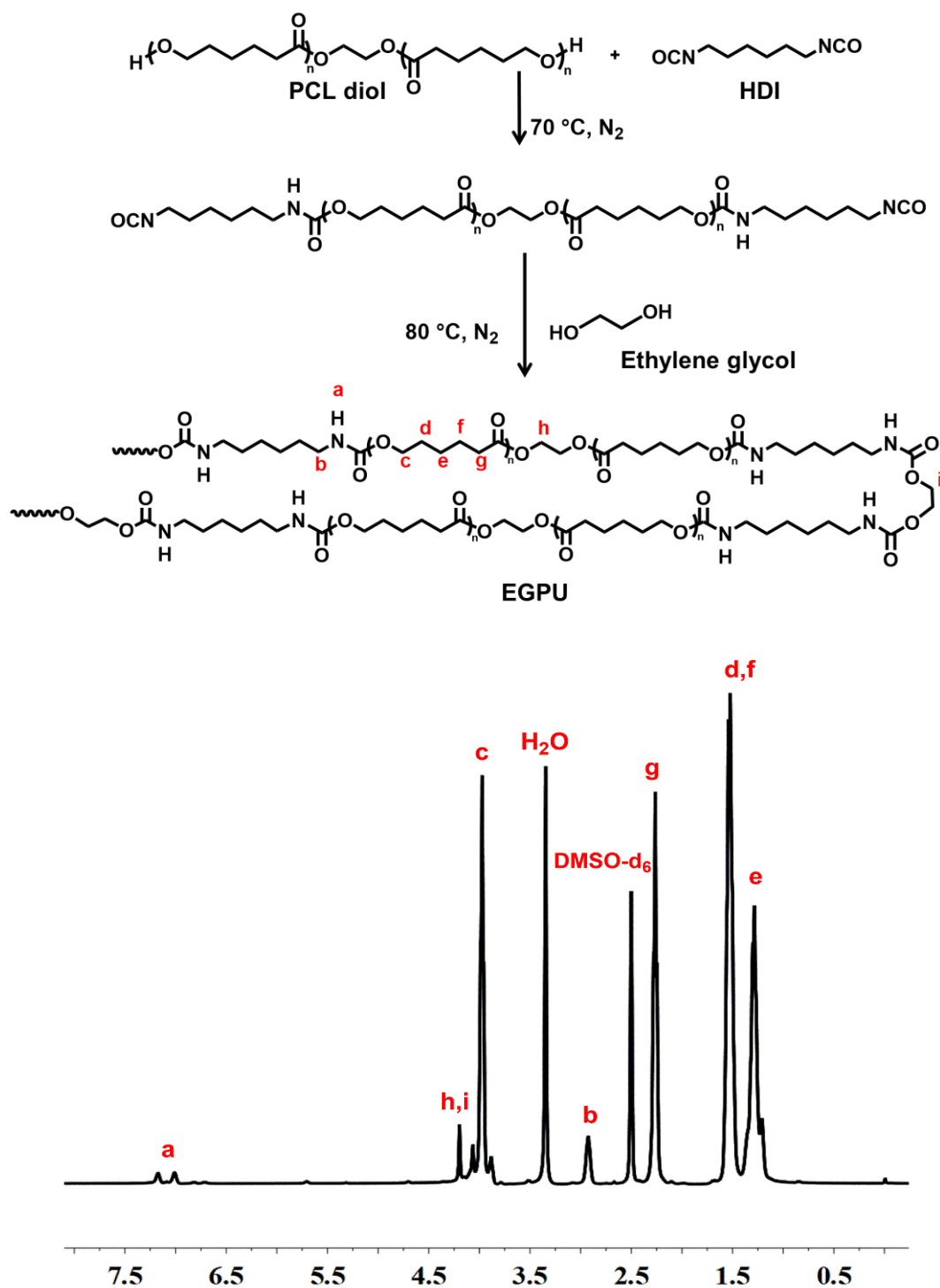


Fig. S6. Synthetic route (top) and ¹H NMR spectrum (bottom) of EGPU in DMSO-d₆ (400 MHz).

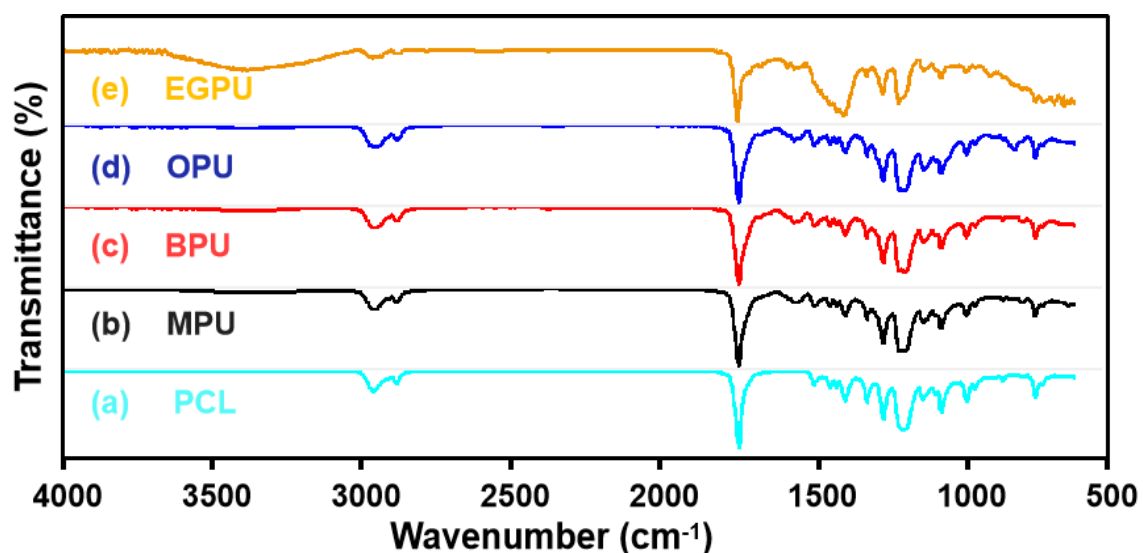


Fig. S7. Graphical analysis of a) PCL-diol, b) MPU, c) BPU, d) OPU and e) EGPU-based elastomers by Fourier transform infrared spectroscopy. Intense bands at 3440 cm^{-1} and 1700 cm^{-1} correspond to -OH and C=O groups in the PCL diol. The peaks at 2940 cm^{-1} and 2860 cm^{-1} belong to -CH_2 symmetric and asymmetric vibrations, respectively. Absorption at 1470 cm^{-1} and 1419 cm^{-1} corresponds to various modes of C-H bending of CH_2 . The absorption band at 1159 cm^{-1} is due to the C-O bonds, and the peak at 1367 cm^{-1} demonstrates that the C-O bonds are attached to cyclic anhydride. The spectra of three kinds of ionic PUs exhibit absorbance at 1520 cm^{-1} , which is assigned to the newly formed amino groups. Additionally, the absorption peak at 1722 cm^{-1} is derived from -CONH- in the PU spectrum. Furthermore, the disappearance of the isocyanate group at 2272 cm^{-1} indicates the successful incorporation of imidazolium ILs as chain extenders and the successful polymerization of soft segments of PCL-diols in PUs.

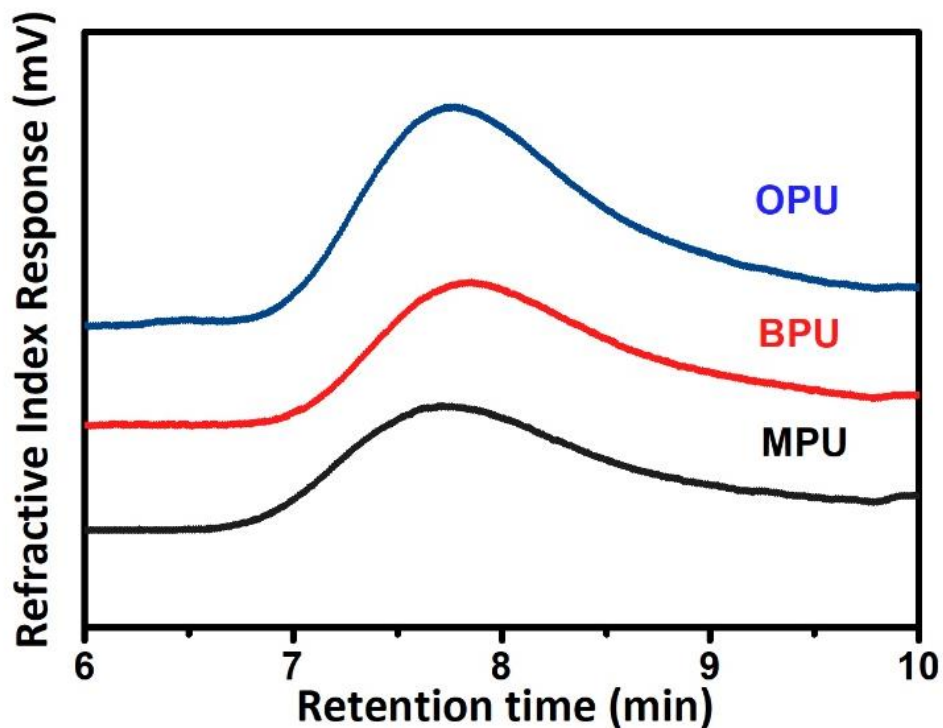


Fig. S8. THF-GPC profiles of synthesized ionic PUs, MPU, BPU, and OPU. Molecular weight and polydispersity (PDI) values of ionic PUs were determined by a TOSOH HLC-8320 size exclusion chromatograph (SEC) equipped with refractive-index and UV detectors using two TSK gel Super Multipore HZ-N (4.6×150 mm, $3 \mu\text{m}$ bead size) columns arranged in series with a molecular weight separation ranging from 500 to 1.9×10^5 g mol⁻¹. DMF containing 10 mM LiBr was used as the eluent. Data acquisition was performed using EcoSEC software and calibrated with polystyrene (PS) standards.

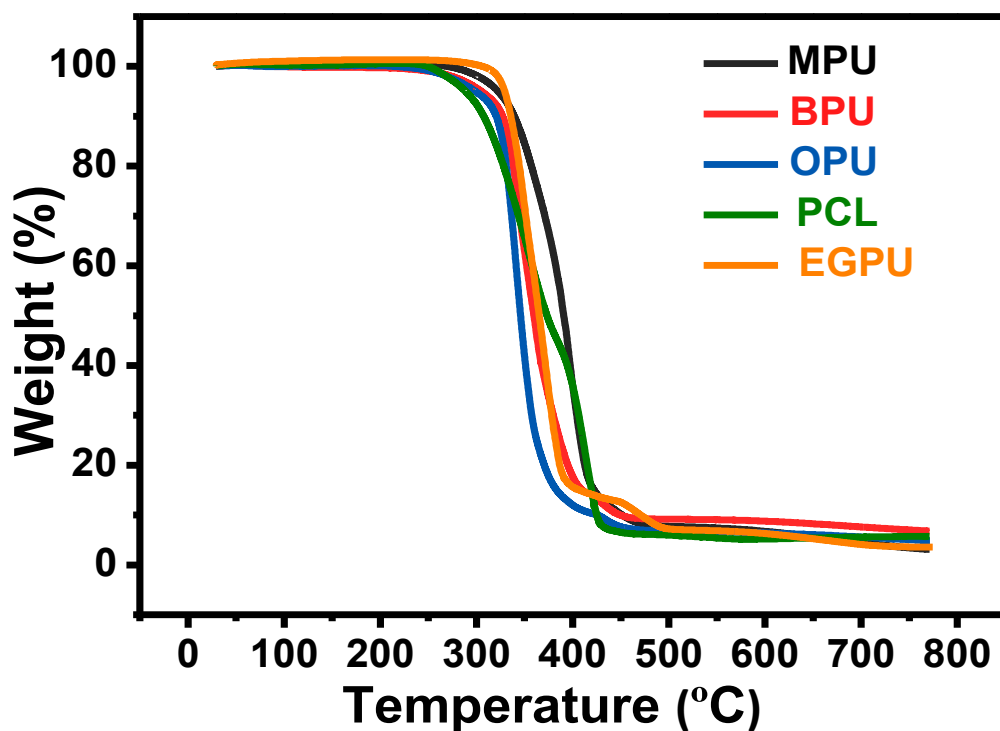


Fig. S9. Thermogravimetric analysis (TGA) was performed using a Universal Analysis 2000 thermogravimetric analyzer under a N₂ atmosphere from 30 °C to 800 °C with a heating rate of 20 °C min⁻¹. It can be seen that all PUs exhibited T_d (T_d: onset decomposition temperature corresponding to the temperature with a percentage weight loss of approximately 5%) at approximately 300 °C.

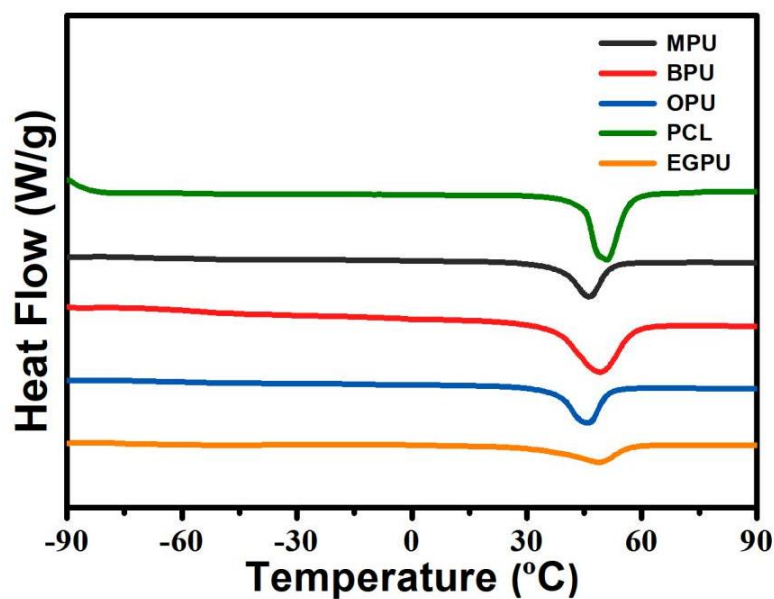


Fig. S10. Differential scanning calorimetry (DSC) analysis was recorded using a TA DSC2010 equipped with a refrigerated cooling system and nitrogen as the purge gas. Samples were heated from -100 °C to 100 °C at a heating rate of 10 °C min⁻¹. The second heating run curves of three ionic PUs show sharp endothermic peaks at approximately 37 °C, corresponding to the melting temperature of PCL crystallization (T_m).

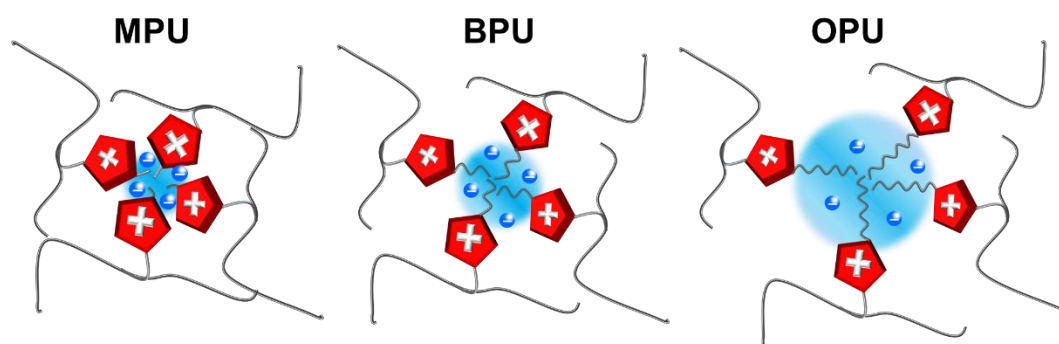
Table S1. Molecular weights, molecular weight distributions, and melting and decomposition temperatures for the PUs investigated in this work.

Sample	M_n	M_w	PDI	T_m	T_d
	(g mol ⁻¹)	(g mol ⁻¹)		(°C)	(°C)
EGPU	65,000	111,800	1.720	39.2	322.4
MPU	24,000	40,100	1.672	37.0	305.1
BPU	11,100	26,700	2.420	37.8	298.7
OPU	11,400	30,300	2.644	33.7	329.1

Table S2. Ultimate tensile stress (UTS), elongation at break, toughness, and recovery percentages of ionic PUs (virgin and cut and replaced ionic PU membranes after 2 h healing at 40 °C).

	Entry	MPU	BPU	OPU
Virgin sample	UTS (MPa)	16.9 ± 0.10	11.6 ± 0.06	9.6 ± 0.11
	Elongation at break (%)	1616 ± 103	1533 ± 120	1467 ± 109
	Toughness (MJ m ⁻³)	198 ± 17	138 ± 15	96 ± 8
Cut and replaced after 2 h at 40°C	UTS (MPa)	11.8 ± 0.05	10.5 ± 0.03	8.9 ± 0.04
	Recovery of UTS (%)	69.7 ± 0.30	90.3 ± 0.2	92.3 ± 0.6
	Elongation at break (%)	922 ± 60	1273 ± 45	1353 ± 97
	Recovery of elongation (%)	57 ± 3	82 ± 4	92 ± 6
	Toughness (MJ m ⁻³)	79 ± 5	111 ± 9	87 ± 11
	Recovery of toughness (%)	40 ± 6	81 ± 9	91 ± 3

Scheme S2. The hypothetical ionic cluster formation for three ionic PUs



The hypothetical ionic cluster formation for ionic PUs

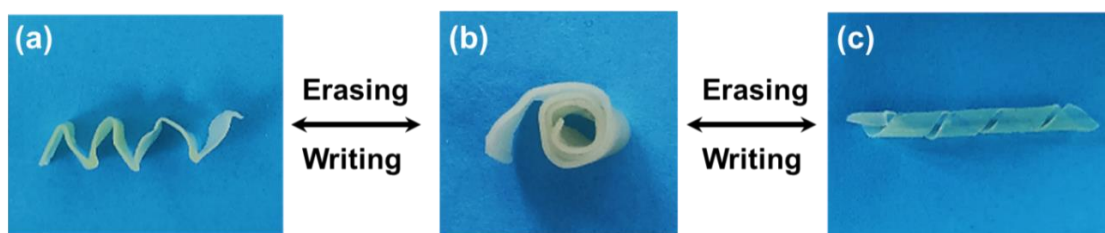


Fig. S11. Varied shapes of a single MPU sample fixed by sequential heating-cooling cycles. (a) Initially, the sample is written into a zigzag shape. (b) The zigzag shape was erased by heating to 60 °C, and the sample was rewritten into a spiral shape. (c) The spiral shape was erased, and a spring shape was obtained using the same procedure.

Table S3. Antibacterial rates for ionic PU membranes and Relative growth rates (RGR) of human dermal fibroblast cells on ionic PU membranes as detected by MTT assay.

Sample	Antibacterial rate (%)		RGR (%)
	<i>E. coli</i>	<i>S. aureus</i>	
MPU	63.19 ± 0.05	99.99 ± 0.01	78.0 ± 1.8
BPU	99.99 ± 0.01	99.99 ± 0.01	75.1 ± 1.2
OPU	99.99 ± 0.01	99.99 ± 0.01	47.5 ± 0.8

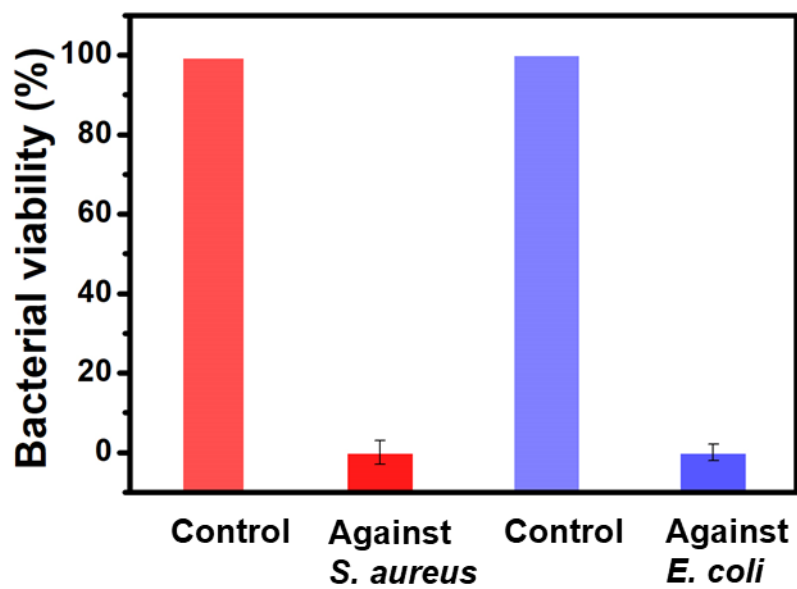


Fig. S12. Bacterial viabilities of *S. aureus* and *E. coli* after contacting with recycled BPU medical gauze for 4 h, with PET membranes as the control. The recycled gauze still exhibited high antibacterial activities.